

# An In-Circuit Noncontacting Measurement Method for $S$ -Parameters and Power in Planar Circuits

Jörgen Stenarson, *Student Member, IEEE*, Klas Yhland, and Claes Wingqvist

**Abstract**—A method for measuring the reflection coefficient and absolute power in the propagating waves from a circuit embedded in a planar circuit environment is presented. The method utilizes a pair of inductive and capacitive probes. The standard one-port vector-network-analyzer calibration is extended to allow the measurement of power in the forward and backward waves. Experimental results are presented for measurements between 700 MHz and 20 GHz. Good agreement between the new noncontacting method and a standard coaxial measurement method is demonstrated up to 12 GHz for power and up to 14 GHz for the reflection coefficient. The method is useful for in-circuit testing of open transmission-line structures, e.g., microstrip.

**Index Terms**—Electromagnetic probe, microwave circuit testing, power measurement, scattering-parameter measurement, vector network analyzer.

## I. INTRODUCTION

**I**N MICROWAVE circuit design and testing, there is a need for  $S$ -parameter and power measurements on system sub-circuits when the system is fully assembled. While it is easy to disconnect and measure sub-circuits with coaxial interfaces, this becomes difficult when the entire system is integrated on a single circuit board. If  $S$ -parameters or power is to be measured for the sub-circuits on the circuit board, it is often necessary to cut the circuit board into pieces. Another approach is to use coplanar probes to contact the sub-circuits. This method also requires physical modification of the system, temporarily cutting the transmission lines connecting the device-under-test (DUT).

Therefore, it is desirable to switch to a noncontacting technique. By applying the test signal through the normal signal path of the system and measure the signal with noncontacting probes, it is possible to measure the  $S$ -parameters and power waves directly.

For  $S$ -parameters, two such methods have been reported. The first method is based on electrooptic probing. It utilizes the field-dependent refractive index (Pockels effect) of a substrate, e.g., GaAs, to measure the field amplitude around a transmission line [1]. The second method uses capacitive probes or in-

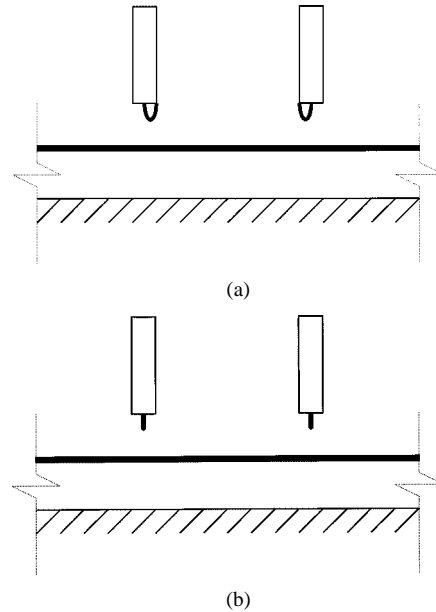


Fig. 1. (a) Capacitive probe configuration. (b) Inductive probe configuration for measuring the waves on a transmission line. This figure shows a side view of the probes as positioned along the transmission line.

ductive probes (Fig. 1) [2]–[6]. There are several drawbacks to these methods. The first method requires complicated laser equipment usually not available in a microwave laboratory. Both methods have the disadvantage that the probing has to be done either using two probes separated by a certain distance or by moving a single probe to two locations to allow the calculation of the propagating waves. Ideally this separation should be a quarter-wavelength. This is inconvenient when measuring over a wide frequency band, as it requires probe movement during the sweep. There is seldom much space between sub-circuits on a circuit board, thus, low-frequency measurements become difficult with these methods.

Neither of the noncontacting methods noted above offer a straightforward means for absolute power measurements.

This paper is an extension of the results presented in [7], where a method to solve the aforementioned drawbacks is presented. By using one inductive and one capacitive probe (Fig. 2), the need for a quarter-wavelength separation of the probes is circumvented. In fact, the probes should be placed as close together as possible since the probe spacing sets the upper frequency limit for this configuration. A straightforward method for absolute power measurement in a planar circuit environment is also presented. Via an adapter removal calibration, an absolute power measurement is transferred from the coaxial environment

Manuscript received March 30, 2001; revised August 24, 2001. This work was supported by the Swedish National Testing and Research Institute and by the Swedish Foundation for Strategic Research.

J. Stenarson is with the Microwave Electronics Laboratory, Chalmers University of Technology, 412 96 Göteborg, Sweden.

K. Yhland is with the SP Swedish National Testing and Research Institute, 501 15 Borås, Sweden and is also with the Microwave Electronics Laboratory, Chalmers University of Technology, 412 96 Göteborg, Sweden.

C. Wingqvist is with the SP Swedish National Testing and Research Institute, 501 15 Borås, Sweden.

Publisher Item Identifier S 0018-9480(01)10428-X.

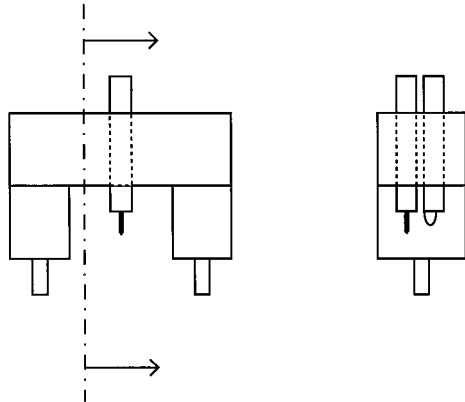


Fig. 2. Fixture for the proposed solution with one capacitive and one inductive probe.

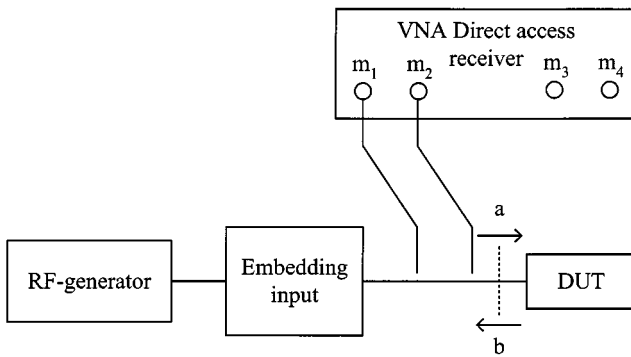


Fig. 3. VNA test setup block diagram for noncontacting measurements.

to the planar circuit environment and, thus, allows for an absolute power calibration of the system. Power correction methods similar to the one used here are presented in [8]–[10].

## II. GENERAL PROCEDURE

A simplified block diagram of the one-port vector network analyzer (VNA) setup used for the noncontacting measurements is shown in Fig. 3. This setup is very similar to a normal VNA. The main difference is that, instead of connecting the receivers of the VNA to the internal couplers, they are connected directly to the probes that measure the current and voltage on the transmission line. The fact that the current and voltage are measured instead of forward and reverse waves is not a problem. Since the current and voltage are linear combinations of the forward and reverse waves, this is taken care of automatically by applying a standard VNA error correction procedure. Another difference is that the RF signal is applied through the embedding circuits of the system during testing and through a connector during calibration (Fig. 3). This means that the embedding impedance for the DUT is different from the embedding impedance of the calibration standards. However, there is no need to know the embedding impedance since the impedance of a one-port can be calculated from the voltage over and current through the one-port without knowing the source impedance.

When using the conventional VNA calibration procedure, there is no information available on the absolute power levels

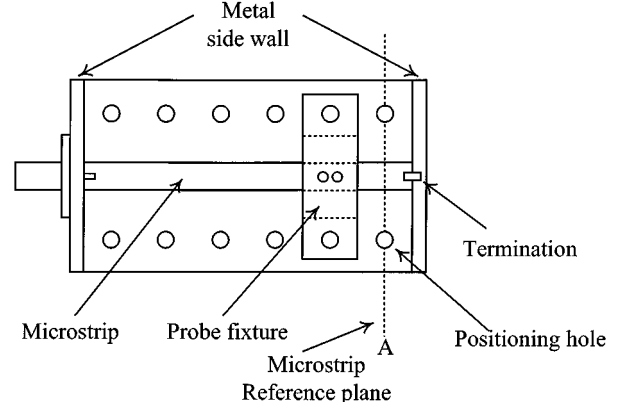


Fig. 4. Test circuit for  $S$ -parameter measurement verification. Microstrip line with terminations short, open, load, and DUT.

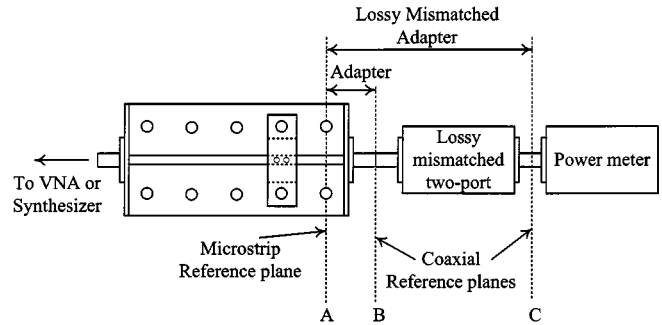


Fig. 5. Test circuit for power measurement verification.

present at the DUT. Normally this is not a problem because the device is measured standalone at a well-defined interface, e.g., coaxial connectors, where it is easy to control the power level. The conventional VNA calibration procedure can be augmented with an extra step for power calibration. A power measurement is then used to adjust the error coefficients of the VNA so that power corrected waves can be calculated.

The complete calibration is a two-step procedure. The first step is the conventional one-port calibration for the microstrip reference plane using three standards. Fig. 4 shows the design of the standards. The second step is power calibration. It is comprised of an adapter characterization and a power measurement that is transferred from the coaxial reference plane to the microstrip plane. The adapter is the part between the microstrip reference plane A and the coaxial reference plane B (Fig. 5).

## III. PROBE AND TEST SUBSTRATE DESIGN

The pair of probes manufactured for the verification of the method contains one capacitive probe [see Fig. 1(a)] and one inductive probe [see Fig. 1(b)]. The inductive probe couples mainly to the magnetic field, which is a measure of the current in the transmission line. The capacitive probe, on the other hand, couples mainly to the electric field surrounding the transmission line and, thus, gives a measure of the voltage on the transmission line.

The capacitive probe is manufactured from a piece of standard 0.085-in semirigid subminiature A (SMA)-type coaxial cable. The outer conductor and dielectric was cut away and a

short piece of the center conductor is used as a probe. The inductive probe was made in a similar way, but a longer piece of center conductor was stripped to allow the folding into a loop. The end of the center conductor was soldered to the outer conductor.

A simple probe fixture was designed (Fig. 2), which allows manual adjustment of the height of the probes above the transmission line. This is, however, meant to be used as a means of adjusting the coupling before the calibration-measurement cycle begins. It is imperative that the relative height remains constant during the cycle because the position is included in the correction factors. Two holes on each side of the transmission line are used to guide the positioning pins (Fig. 4) of the probe fixture. It is important that the holes are accurately positioned relative to the transmission line and the calibration reference plane. To allow some flexibility in the choice of reference plane, several pairs of holes were placed along the transmission line (Fig. 4).

The microstrip test circuits were manufactured on a Rogers RT/Duroid 5870 substrate with  $\epsilon_r = 2.33$  and a thickness of 0.38 mm giving a  $50\text{-}\Omega$  linewidth of 1.11 mm (Fig. 4). A coaxial connector is attached to one end of the microstrip line. It is used to connect the RF source or a VNA. The other end is terminated with a calibration standard, or a DUT. For the microstrip calibration kit, the terminations are short, open, and  $50\text{-}\Omega$  load (SOL), the DUT is a  $24\text{-}\Omega$  resistor. The short was made by soldering a piece of wire from the microstrip line to the sidewall of the fixture, the open by just leaving the end of the line open, and finally, the load was made by soldering two  $100\text{-}\Omega$  surface mount resistors in parallel to the sidewall.

A fourth test circuit with coaxial connectors at both ends was also made (Fig. 5). This circuit is used for the power calibration and verification.

#### IV. CALIBRATION

In this section, we first give a method for calibration of *S*-parameters and power in the case where the power meter can be connected directly to the reference plane of interest, e.g., a coaxial interface. Second, this method is extended to allow calibration at a reference plane, e.g., microstrip, where the power meter must be connected via an adapter.

##### A. *S*-Parameter and Direct Power Calibration

The most common approach to error correction is by modeling the VNA as a linear two-port. A useful review of the VNA calibration subject can be found in [11]. The signals measured by the VNA are designated  $m_1$  and  $m_2$ , the actual waves at the reference plane are designated  $a$  and  $b$  (Fig. 6). The two-port can be thought of as any ordinary two-port, e.g., *S*-, *T*-, or *Y*-parameters. The two-port matrix elements are called error coefficients. *T*-parameters (1) are a natural choice when power correction is to be included as follows:

$$\begin{bmatrix} a \\ b \end{bmatrix} = \begin{bmatrix} T_{11} & T_{12} \\ T_{21} & T_{22} \end{bmatrix} \begin{bmatrix} m_1 \\ m_2 \end{bmatrix}. \quad (1)$$

This equation relates the VNA measurements to the actual waves directly. If the complete *T*-matrix is known,  $a$  and  $b$  can

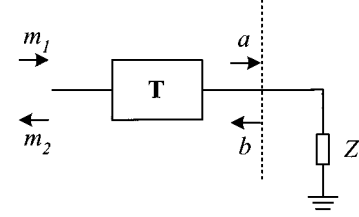


Fig. 6. Model used for *S*-parameter and direct power calibration.

be calculated from  $m_1$  and  $m_2$ , and the reflection coefficient is then calculated by dividing  $b$  by  $a$  as follows:

$$\Gamma = \frac{b}{a} = \frac{T_{21}m_1 + T_{22}m_2}{T_{11}m_1 + T_{12}m_2}. \quad (2)$$

If we substitute the ratio of  $m_2$  to  $m_1$  by  $M$ , this gives

$$\Gamma_x = \frac{T_{21} + T_{22}M_x}{T_{11} + T_{12}M_x} = \frac{T_{21}/T_{11} + T_{22}/T_{11}M_x}{1 + T_{12}/T_{11}M_x} \quad (3)$$

where  $\Gamma_x$  is the reflection coefficient of the termination. The standard calibration procedure is to measure  $M_x$  for three different terminations, e.g., SOL, where the letter subscript of the variables is used to denote which standard is used. Rearranging (3) for these three measurements gives the calibration coefficient equation

$$\begin{bmatrix} M_S\Gamma_S & -1 & -M_S \\ M_O\Gamma_O & -1 & -M_O \\ M_L\Gamma_L & -1 & -M_L \end{bmatrix} \begin{bmatrix} T_{12}/T_{11} \\ T_{21}/T_{11} \\ T_{22}/T_{11} \end{bmatrix} = \begin{bmatrix} -\Gamma_S \\ -\Gamma_O \\ -\Gamma_L \end{bmatrix} \quad (4)$$

and, thus, the error coefficients, normalized to  $T_{11}$ , are known as follows:

$$\mathbf{T}' = \begin{bmatrix} 1 & T_{12}/T_{11} \\ T_{21}/T_{11} & T_{22}/T_{11} \end{bmatrix}. \quad (5)$$

As can be seen from (3), the normalized error coefficients  $\mathbf{T}'$  are sufficient for reflection coefficient measurement. The magnitude of  $T_{11}$  is necessary when measuring the absolute power waves  $a$  and  $b$ . The phase of  $T_{11}$  is not necessary for any measurement.

The magnitude of  $T_{11}$  is determined by measuring the power absorbed by a load at the reference plane

$$P = |a_P|^2 - |b_P|^2. \quad (6)$$

Using (1) and (6) gives (7), shown at the bottom of the following page. After this step, all four error coefficients are known as follows:

$$\mathbf{T} = |T_{11}|\mathbf{T}' \quad (8)$$

and it is now possible to calculate the power corrected  $a$  and  $b$  from (1).

##### B. Transferred Power Calibration

Since it is difficult to measure the power directly at a microstrip reference plane, a transferred power measurement is used for the calibration. The test circuit in Fig. 5 with coaxial connectors in both ends is used for this transfer calibration. The calibration model used is shown in Fig. 7, where  $\mathbf{T}_e$  contains the

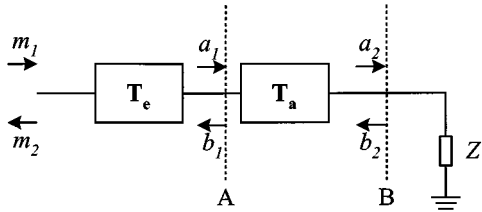


Fig. 7. Model used for  $S$ -parameter and transferred power calibration.

error coefficients for the calibration to reference plane A and  $\mathbf{T}_a$  is the adapter between A and B.

The adapter is characterized by an adapter removal calibration. This requires the normalized error coefficients  $\mathbf{T}'_e$  to be known from a SOL calibration at reference plane A. The adapter characterization is done in two steps. First, the normalized  $T$ -parameters of the adapter  $\mathbf{T}'_a$  are calculated from a standard SOL calibration between reference planes A and B. Second,  $\mathbf{T}_a$  is determined from  $\mathbf{T}'_a$  by the added constraint that the adapter is a reciprocal network

$$\mathbf{T}_a = \frac{\mathbf{T}'_a}{\sqrt{\det(\mathbf{T}'_a)}}. \quad (9)$$

Now that  $\mathbf{T}_a$  is known, the power  $P_A$  delivered to reference plane A is given by

$$P_A = \frac{1 - |\Gamma_A|^2}{|T_{a,11} + T_{a,12}\Gamma_A|^2 - |T_{a,21} + T_{a,22}\Gamma_A|^2} P_B \quad (10)$$

where  $P_B$  is the power measured at reference plane B, and  $\Gamma_A$  is the reflection coefficient measured at A when the power meter is connected at B.

Since  $P_A$  is now known, this allows the complete determination of  $\mathbf{T}_e$  from (7) and (8).

## V. EXPERIMENTAL VERIFICATION

### A. Verifying the $S$ -Parameter Measurement Method

To verify the accuracy of the method, one can choose several different paths. The best way is, of course, to compare the measurements to a known well-defined verification standard. Such a standard was not available for the microstrip substrates used here. Rather than developing high-performance calibration standards, a calibration is performed through the coaxial connector using exactly the same standards. Thus obtaining a verification of the noncontacting measurement technique, by the comparison to a standard coaxial measurement. The verifying measurement was done using a conventional testset (Agilent 8517B) with the VNA Agilent 8510C.

The main contributor to measurement errors for the coaxial calibration and measurement, relevant to this comparison, is the coaxial-to-microstrip transition repeatability and similarity. It turned out to be a major problem for accurate measurements. Using the time-gating option of the Agilent 8510C, it is pos-

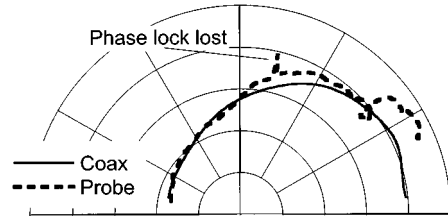


Fig. 8. Reflection coefficient of a 24- $\Omega$  resistor measured with noncontacting probe (---), coaxial (—), 0.7–20 GHz.

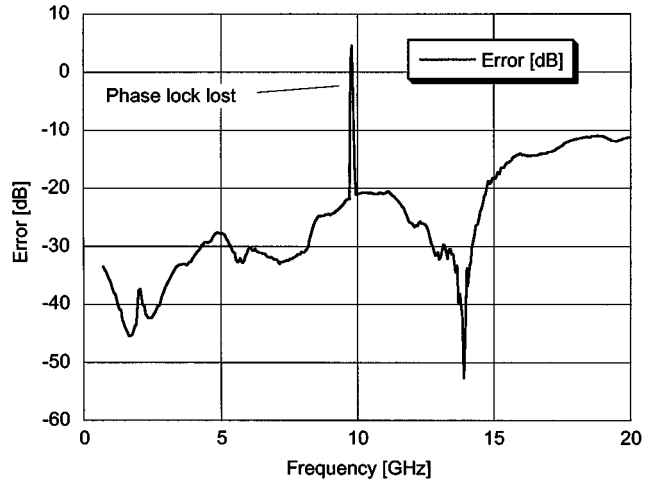


Fig. 9. Magnitude of error vector between noncontacting probe and coaxial measurements.

sible to minimize this problem. For the noncontacting calibration case, it is the repeatability of probe positioning that is the key contributor to errors. The probe to microstrip distance and the probe position transversal to the microstrip length axis are especially important since they determine the coupling between the probe and microstrip line. The position along the microstrip axis gives a phase error. The DUT used for comparing noncontacting and coaxial measurements was made from a 24- $\Omega$  resistor. The results shown in Figs. 8 and 9 give a good agreement up to about 14 GHz for the  $S$ -parameters. At approximately 10 GHz, there is a glitch in the curve caused by a phase-lock problem due to weak coupling for the probe connected to the reference channel of the direct access receiver (Agilent 8511B). This problem occurs when the distance to a short or open is such that there is a minimum of the voltage or current on the line for the capacitive and inductive probe, respectively. This is a problem for all devices with a high reflection coefficient, which are usually the calibration standards. For the particular pair of probes used here, the voltage coupling is more sensitive due to a deeper null in the coupling.

### B. Verifying the Power Measurement Method

The noncontacting power measurements were also verified by a comparison to measurements performed through a coaxial

$$|T_{11}| = \sqrt{\frac{P}{|m_{1,P} + m_{2,P}T_{12}/T_{11}|^2 - |m_{1,P}T_{21}/T_{11} + m_{2,P}T_{22}/T_{11}|^2}} \quad (7)$$

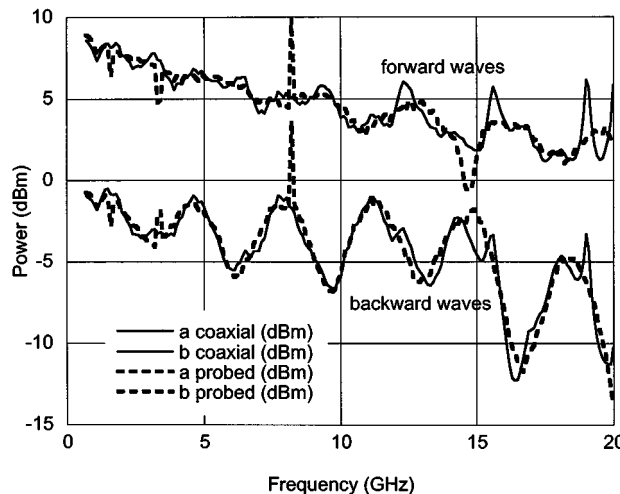


Fig. 10. Comparison of forward and backward power waves for noncontacting probe (---) and verifying coaxial (—) measurement.

interface. For this case, a DUT quite different from the one used for *S*-parameter verification was used. The basic setup is shown in Fig. 5, i.e., a lossy mismatched two-port has been inserted between the power meter and the test circuit board. With the microstrip-to-coaxial transition, this two-port forms a lossy and mismatched adapter. The purpose of the two-port is to provide a mismatched load at the microstrip reference plane and a convenient means for the verifying power measurement.

If the *T*-parameters of the lossy adapter and the reflection coefficient at the microstrip reference plane of the new DUT are known, the magnitudes of the incident and reflected waves at the microstrip reference plane can be calculated from the reading of the power meter and, thus, provide a verifying measurement. The *T*-parameters of the lossy adapter were determined from time-gated measurements through the coaxial connector of the two-port carrier using a conventional VNA testset (8517B) with the 8510C. For this purpose, an adapter removal procedure is employed (for details, see Section IV).

The power wave measurements agree well with the verifying measurements (Fig. 10). The difference between the noncontacting measurements and the verifying measurement is shown in Fig. 11. The data shows less than 0.8-dB difference up to about 12 GHz, except at the indicated glitches that represent phase-lock problems. As can be expected, this measurement is not as exact as the ordinary reflection measurement since the power measurement needs the results for the backward and forward wave independently. This means that a change in coupling will result in an error in measured power. On the other hand, when measuring the reflection coefficient, this problem tends to cancel because the error in power for both waves is correlated.

There are more glitches in the power curve than in the reflection measurement (Fig. 12). This is due to the two-step calibration procedure, where the adapter removal calibration has different frequencies with phase-lock problems since the distance to the short and open is different and, thus, the minima for the voltage and current occur at different frequencies. There could also be glitches from phase-lock problems during the measurement, however this only occurs when measuring DUTs with a high reflection.

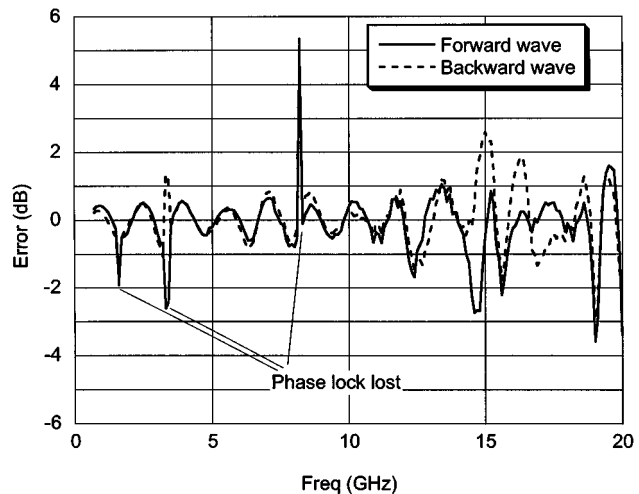


Fig. 11. Error between noncontacting probe and coaxial measured power waves.

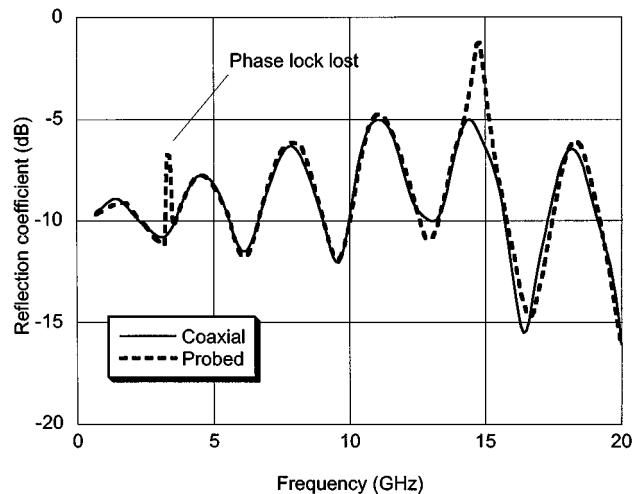


Fig. 12. Reflection coefficient at microstrip reference plane for noncontacting probe (---) and verifying coaxial measurement (—).

## VI. DISCUSSION AND RESULTS

The presented method shows great promise for in-circuit testing where either reflection or power measurements are required. This has previously required physical modification or even complete disassembly in order to test sub-circuits in a microstrip environment. The method has been demonstrated for one-port measurement, but is extendable to two-ports as well. The power calibration is, in principle, only required on one of the ports because the thru standard in two-port calibrations facilitates the transfer of power correction to the second port.

In order to deploy the method in a production environment, there is a need for more research and development. The probes need to be improved to increase positioning accuracy, as well as electrical performance. The accuracy of the system needs to be evaluated. Sensitivity to probe positioning errors is an especially important topic for the design of the probe system. There are also unanswered questions regarding how close the probes can be placed to the DUT and still function properly. This will set limits on the necessary spacing between components to be tested.

## ACKNOWLEDGMENT

The authors would like to thank H. Nilsson, SP, Borås, Sweden, and M. Tibell, Swedish Metrology Council, for their encouragement. The authors further thank S. Davidsson, Chalmers University of Technology, Göteborg, Sweden, C. Fager, Chalmers University of Technology, Göteborg, Sweden, N. Rorsman, Chalmers University of Technology, Göteborg, Sweden, J. P. Starski, Chalmers University of Technology, Göteborg, Sweden, and H. Zirath, Chalmers University of Technology, Göteborg, Sweden, for helpful discussion and comments.

## REFERENCES

- [1] G. David, W. Schroeder, D. Jager, and I. Wolff, "2D electro-optic probing combined with field theory based multimode wave amplitude extraction: A new approach to on-wafer measurement," in *IEEE MTT-S Int. Microwave Symp. Dig.*, 1995, pp. 1049–1052.
- [2] G. Yingjie and I. Wolff, "A new miniature magnetic field probe for measuring three-dimensional fields in planar high-frequency circuits," *IEEE Trans. Microwave Theory Tech.*, vol. 44, pp. 911–918, June 1996.
- [3] ——, "A miniature magnetic field probe for measuring fields in planar high-frequency circuits," in *IEEE MTT-S Int. Microwave Symp. Dig.*, 1995, pp. 1159–1162.
- [4] ——, "Measurements of field distributions and scattering parameters in multiconductor structures using an electric field probe," in *IEEE MTT-S Int. Microwave Symp. Dig.*, 1997, pp. 1741–1744.
- [5] S. S. Osofsky and S. E. Schwarz, "A noncontacting probe for measurements on high-frequency planar circuits," in *IEEE MTT-S Int. Microwave Symp. Dig.*, 1989, pp. 823–825.
- [6] ——, "Design and performance of a noncontacting probe for measurements on high-frequency planar circuits," *IEEE Trans. Microwave Theory Tech.*, vol. 40, pp. 1701–1708, Aug. 1992.
- [7] J. Stenarson, K. Yhland, and C. Wingqvist, "An in-circuit, noncontacting, *S*-parameter measurement method for planar circuits," presented at the ARFTG 57th Microwave Meas. Conf., Phoenix, AZ, 2001.
- [8] A. Ferrero and U. Pisani, "An improved calibration technique for on-wafer large-signal transistor characterization," *IEEE Trans. Instrum. Meas.*, vol. 42, pp. 360–364, Apr. 1993.
- [9] B. Hughes, A. Ferrero, and A. Cognata, "Accurate on-wafer power and harmonic measurements of mm-wave amplifiers and devices," in *IEEE MTT-S Int. Microwave Symp. Dig.*, 1992, pp. 1019–1022.
- [10] B. Roth, D. Kother, T. Sporkmann, W. Lutke, I. Wolff, and R. G. Ranson, "Vector corrected on-wafer power measurements of frequency converting two-ports," in *IEEE MTT-S Int. Microwave Symp. Dig.*, 1996, pp. 1281–1284.
- [11] B. Schiek, "Developments in automatic-network analyzer calibration methods," in *Review of Radio Science 1993–1996*, W. R. Stone, Ed. Oxford, U.K.: Oxford Univ. Press, 1996, vol. 1, pp. 115–155.

**Jörgen Stenarson** (S'98) received the M.Sc. degree in engineering physics from the Chalmers University of Technology, Göteborg, Sweden, in 1997, and is currently working toward the Ph.D. degree in microwave electronics at the Chalmers University of Technology.

His research interests are noncontacting *S*-parameter measurement, FET noise models, noise model extraction methods, and low-noise amplifier design.

**Klas Yhland** received the M.Sc. degree in electronic engineering from the Lund University of Technology, Lund, Sweden, in 1992, and the Ph.D. degree in microwave electronics from the Chalmers University of Technology, Göteborg, Sweden, in 1999.

From 1992 to 1994, he was with the Airborn Radar Division, Ericsson Microwave Systems. Since 1999, he has been in charge of the National Laboratory for High Frequency and Microwave Measurements, SP Swedish National Testing and Research Institute, Borås, Sweden. He is also with the Microwave Electronics Laboratory, Chalmers University of Technology.

**Claes Wingqvist**, photograph and biography not available at time of publication.